Editors' Suggestion

Confinement-induced resonances for the creation of quasi-one-dimensional ultracold gases of alkali-alkaline-earth dimers

Lorenzo Oghittu , 1,2 Premjith Thekkeppatt , 3,4 Nirav P. Mehta , 1,5,6 Seth T. Rittenhouse , 1,6,7 Klaasjan van Druten , 2,3 Florian Schreck, 2,3 and Arghavan Safavi-Naini, 2

¹Institute for Theoretical Physics, Institute of Physics, University of Amsterdam, Science Park 904, 1098 XH Amsterdam, The Netherlands ²QuSoft, Science Park 123, 1098 XG Amsterdam, The Netherlands

³Van der Waals-Zeeman Institute, Institute of Physics, University of Amsterdam, 1098 XH Amsterdam, The Netherlands ⁴NNF Quantum Computing Programme, Niels Bohr Institute, University of Copenhagen, Blegdamsvej 17, 2100 Copenhagen, Denmark ⁵Department of Physics and Astronomy, Trinity University, San Antonio, Texas 78212, USA

⁶ITAMP, Center for Astrophysics, Harvard & Smithsonian, 60 Garden Street, Cambridge, Massachusetts 02138, USA ⁷Department of Physics, U.S. Naval Academy, Annapolis, Maryland 21402, USA

(Received 11 June 2025; accepted 12 September 2025; published 14 October 2025)

We theoretically investigate the role of confinement-induced resonances (CIRs) in low-dimensional ultracold atomic mixtures in the formation of weakly bound dimers. To this end, we examine the scattering properties of a binary atomic mixture confined by a quasi-one-dimensional (quasi-1D) potential. In this regime, the interspecies two-body interaction is modeled as an effective 1D zero-range pseudopotential, with a coupling strength g_{1D} derived as a function of the three-dimensional scattering length a. This framework enables the study of CIRs in harmonically confined systems, with particular attention paid to the case of mismatched transverse trapping frequencies of the two atomic species. Finally, we consider the Bose-Fermi mixture of ⁸⁷Rb and ⁸⁷Sr and identify values of the experimentally accessible parameters for which CIRs can be exploited to create weakly bound molecules.

DOI: 10.1103/3m6z-t6pb

I. INTRODUCTION

Ultracold gases of polar molecules have emerged as a rapidly advancing field of research [1]. Owing to their long-range, anisotropic dipole-dipole interactions, these systems offer a highly versatile platform for a wide range of applications, including quantum simulation [2], precision measurement [3,4], and quantum chemistry [5]. However, the creation of an ultracold gas of dipolar molecules poses significant challenges. Experimentally, two methods for creating ultracold gases of ground-state molecules are commonly employed. The first consists of starting with a thermal gas of molecules and cooling it down via laser techniques [6–8]. Yet, the complicated internal, electronic, rotational, and vibrational structure of the molecules can limit their ability to scatter enough photons, often making laser cooling ineffective for many molecular species [9]. The second method involves starting from an ultracold gas of unbound atoms and associating them to weakly bound molecules through adiabatic passage across a resonance. These weakly bound molecules can then be directly associated to their rovibrational ground state via stimulated Raman adiabatic passage [10-12]. Forming the initial gas of weakly bound molecules usually requires the system to have a readily accessible broad magnetic Feshbach resonance [13] as seen in many bialkali systems, e.g., K-Rb [10]. Because such broad resonances may not be available in some ultracold mixtures, for example, due to a weak magnetic response of the atoms or the resonance appearing at very large magnetic fields [14], a different approach becomes necessary.

In this work, we theoretically investigate the use of a different kind of resonance as a pathway for creating weakly bound molecules: the confinement-induced resonance (CIR) [15-21]. CIRs arise in ultracold gases when atoms experience a strong confinement along one or more directions that effectively reduces their dynamics to lower-dimensional regimes. Here, we focus on quasi-one-dimensional (quasi-1D) mixtures of alkali and alkaline-earth atoms. The corresponding heteronuclear dimers constitute a particularly interesting system thanks to their sizable electric and magnetic dipole moments [22]. Unlike bialkali dimers, however, the formation of these molecules via magnetoassociation poses considerable challenges. This is primarily due to the nonmagnetic ground state of alkaline-earth atoms, which is responsible for exceedingly narrow Feshbach resonances [23–25]. In this context, the use of CIRs emerges as an appealing alternative. Taking into consideration the relevant Bose-Fermi mixture of ⁸⁷Rb and ⁸⁷Sr confined by a quasi-1D harmonic potential (see Fig. 1), we perform a numerical analysis to characterize the emergence of CIRs. We emphasize that the formation of molecules via two-body CIRs requires a coupling between the center of mass and relative motion, as established in Ref. [19]. In the present case, such coupling is introduced by the mismatch in trapping frequencies between the two atomic species, giving rise to narrow inelastic resonances associated with excited center-of-mass bound states. In light of this mechanism, our investigation ultimately aims to identify suitable values of tunable parameters that could support ongoing experimental efforts toward realizing ultracold ⁸⁷Rb - ⁸⁷Sr dimers.

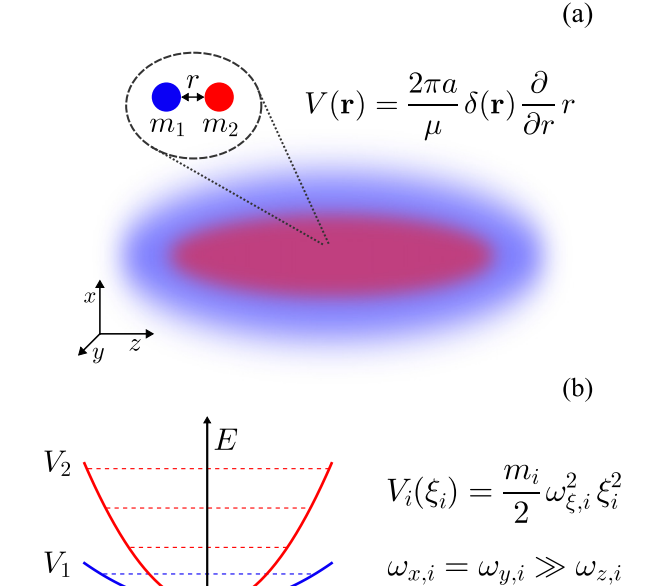


FIG. 1. (a) Scheme of the system: a mixture of two species with masses m_1 and m_2 confined by quasi-one-dimensional potentials with different trapping frequencies. The interspecies interaction is represented by the regularized zero-range pseudopotential V(r), with r being the interparticle distance, μ being the reduced mass, and a being the 3D scattering length. (b) Harmonic potentials along direction $\xi = x, y, z$ for the two species i = 1, 2. Direction z is the direction of weak confinement.

This paper is organized as follows: In Sec. II we describe the two-body problem consisting of one particle of each species interacting via a contact potential. In Sec. III we show how scattering properties are extracted, and we provide explicit expressions for the specific case of harmonic confinement. These two sections closely follow the description in Ref. [17] and are reported here for the sake of completeness. In Sec. IV, we describe how the spectrum is computed in the 1D limit. In Sec. V, we present a numerical analysis based on the previous sections. Some comments on how our results are relevant for ongoing experiments are provided in Sec. VI. Finally, the conclusions and outlook are summarized in Sec. VII.

II. TWO-BODY PROBLEM

A. Hamiltonian and Schrödinger equation

We consider two different atomic species with masses m_1 and m_2 . Each of them is confined by a two-dimensional external potential $V_i(\mathbf{x}_{\perp,i})$, where $\mathbf{x}_{\perp,i} = (x_i, y_i)$ indicates the coordinates of species i along the transversal direction of confinement. The longitudinal coordinate is labeled z_i , and the corresponding confinement is assumed to be negligible. Moreover, we assume that we are in the ultracold regime, where only s-wave scattering is relevant to describe the atomatom interaction. The latter can therefore be modeled by the

zero-range regularized pseudopotential

$$V(\mathbf{r}) = \frac{2\pi a}{\mu} \delta(\mathbf{r}) \frac{\partial}{\partial r} r, \tag{1}$$

where **r** is the separation between the two atoms, μ is the reduced mass, and a is the three-dimensional (3D) intra- or interspecies scattering length. Here and throughout the paper, we set $\hbar = 1$. The Hamiltonian of a system consisting of one particle of each species is

$$H = \sum_{i=1,2} \left[\frac{\mathbf{p}_i^2}{2m_i} + V_i(\mathbf{x}_{\perp,i}) \right] + V(|\mathbf{x}_1 - \mathbf{x}_2|). \tag{2}$$

It is convenient to transform Eq. (2) in the center-of-mass and relative coordinates defined by

$$\mathbf{R} = \frac{m_1 \mathbf{x}_1 + m_2 \mathbf{x}_2}{M}, \quad \mathbf{r} = \mathbf{x}_1 - \mathbf{x}_2, \tag{3}$$

with the corresponding momenta

$$\mathbf{P} = \mathbf{p}_1 + \mathbf{p}_2, \quad \mathbf{p} = \frac{m_2 \mathbf{p}_1 + m_1 \mathbf{p}_2}{M}, \tag{4}$$

where $M = m_1 + m_2$. We note that the longitudinal centerof-mass coordinate is decoupled from the other degrees of freedom because the confinement is purely transversal. Hence, the system is entirely characterized by the set of coordinates $(\mathbf{R}_{\perp}, \mathbf{r})$ or, alternatively, by $(\mathbf{x}_{\perp,1}, \mathbf{x}_{\perp,2}, z)$. Here, \mathbf{R}_{\perp} is the center-of-mass transversal coordinate, while z is the longitudinal relative coordinate. Analogous notation will be adopted for the momenta. The Hamiltonian can be written as

$$H = H_{\parallel} + H_{\perp}^{(1)} + H_{\perp}^{(2)} + V(r), \tag{5}$$

with $H_{\parallel} = p_z^2/(2\mu)$ and

$$H_{\perp}^{(i)} = \frac{p_{\perp}^2}{2m_i} + V_i(\mathbf{x}_{\perp,i}). \tag{6}$$

With the aim of computing the scattering properties of such a system, we start from the two-particle Schrödinger equation,

$$(H_0 - E)\Psi(\mathbf{R}_{\perp}, \mathbf{r}) = -V(\mathbf{r})\Psi(\mathbf{R}_{\perp}, \mathbf{r})$$
$$= \frac{f(\mathbf{R}_{\perp})}{2\mu}\delta(\mathbf{r}), \tag{7}$$

where we defined the noninteracting Hamiltonian $H_0 = H - V$ and, in the last equality, we explicitly took into account the pseudopotential in Eq. (1) by imposing Bethe-Pierls boundary conditions,

$$\Psi(\mathbf{R}_{\perp}, \mathbf{r} \to 0) \simeq \frac{f(\mathbf{R}_{\perp})}{4\pi r} \left(1 - \frac{r}{a}\right).$$
 (8)

The general solution to Eq. (7) can be formally written as

$$\Psi(\mathbf{R}_{\perp}, \mathbf{r}) = \Psi_0(\mathbf{R}_{\perp}, \mathbf{r})$$

$$+ \int_{\mathbb{R}^2} d\mathbf{R}'_{\perp} G_E(\mathbf{R}_{\perp}, \mathbf{r}; \mathbf{R}'_{\perp}, 0) \frac{f(\mathbf{R}'_{\perp})}{2\mu}, \qquad (9)$$

where the first term on the right-hand side is the solution to the homogeneous equation $(H_0 - E)\Psi_0 = 0$, while the second is the particular solution written in terms of the Green's function $G_E = (H_0 - E)^{-1}$. Therefore, all the information on the scattering between the two particles is contained in $f(\mathbf{R}_{\perp})$. Later in the paper, we shall see how to extract it.

Before proceeding, we remark that the energy E indicates the total energy of the system,

$$E = \frac{k^2}{2\mu} + E_{n_1}^{(1)} + E_{n_2}^{(2)},\tag{10}$$

where k is the longitudinal relative momentum and n_i is the transverse quantum number of particle i. States with fixed n_1 and n_2 are referred to as channels, which are said to be open when $E \geqslant E_{n_1}^{(1)} + E_{n_2}^{(2)}$ and closed otherwise.

B. Imaginary-time propagator

Let us write the Green's function of the system as

$$G_E(\mathbf{R}_{\perp}, \mathbf{r}; \mathbf{R}'_{\perp}, 0) = \int_0^\infty dt \, e^{Et} G_t(\mathbf{R}_{\perp}, \mathbf{r}; \mathbf{R}'_{\perp}, 0), \quad (11)$$

with the imaginary-time propagator [26]

$$G_t(\mathbf{R}_{\perp}, \mathbf{r}; \mathbf{R}'_{\perp}, 0) = \langle \mathbf{R}_{\perp}, \mathbf{r} | e^{-H_0 t} | \mathbf{R}'_{\perp}, 0 \rangle.$$
 (12)

According to Eq. (5), we can factorize the longitudinal and transversal contributions. The former is the imaginary-time propagator of a free particle,

$$\langle z|e^{-H_{\parallel}t}|z'\rangle = \left(\frac{\mu}{2\pi t}\right)^{1/2} e^{-(z-z')^2\mu/(2t)},$$
 (13)

while the latter reads

$$\langle \mathbf{x}_{\perp,i} | e^{-H_{\perp}^{(i)} t} | \mathbf{x}_{\perp,i}' \rangle = \sum_{n} e^{-E_{n}^{(i)} t} \psi_{n}^{(i)}(\mathbf{x}_{\perp,i}) \bar{\psi}_{n}^{(i)}(\mathbf{x}_{\perp,i}'), \quad (14)$$

with $\psi_n^{(i)}$ being the eigenstates of $H_{\perp}^{(i)}$ with eigenvalue $E_n^{(i)}$. Hence, we can write Eq. (12) as follows:

$$G_{t}(\mathbf{R}_{\perp}, \mathbf{r}; \mathbf{R}'_{\perp}, 0) = \sqrt{\frac{\mu}{2\pi t}} e^{-z^{2}\mu/(2t)} \prod_{i=1,2} \sum_{n_{i}} e^{-E_{n_{i}}^{(i)}t} \psi_{n_{i}}^{(i)}(\mathbf{x}_{\perp,i}) \bar{\psi}_{n_{i}}^{(i)}(\mathbf{x}'_{\perp,i}).$$
(15)

We observe from the definition in Eq. (12) that the integrand in Eq. (11) decays with $\exp[-E_B t]$ at large times, where $E_B = E_0 - E$ is the binding energy and $E_0 = E_0^{(1)} + E_0^{(2)}$ is the ground-state energy of H_0 . However, the term with $n_1 = n_2 = 0$ gives a contribution to the Green's function proportional to $1/\sqrt{E_B}$ [27], which is divergent when E_B approaches zero. Therefore, as soon as the lowest channel opens at $E = E_0$, it is useful to separate its diverging contribution from that of the closed channels. We do that by substituting the transversal Hamiltonian $H_{\perp,i}$ in Eq. (14) with its projection onto the Hilbert subspace orthogonal to the open channel. In the next section, we indicate with a tilde the operators that require such a precaution. Finally, we note that this approach can be generalized to the case where excited states become energetically open.

III. SCATTERING SOLUTIONS

The aim of this section is to derive solutions to the twobody problem defined above.

A. General results

The incoming state in the two-particle problem is conveniently written as

$$\Psi_0(\mathbf{x}_{\perp,1}, \mathbf{x}_{\perp,2}, z) = e^{ikz} \, \psi_0^{(1)}(\mathbf{x}_{\perp,1}) \psi_0^{(2)}(\mathbf{x}_{\perp,2})
\equiv e^{ikz} \, \psi_0(\mathbf{R}_\perp, \mathbf{r}_\perp),$$
(16)

with $\psi_0^{(i)}$ being the single-particle transversal ground state and $k = \sqrt{2\mu(E - E_0)}$ being the longitudinal relative momentum. We can write the Green's function as

$$G_{E}(\mathbf{R}_{\perp}, \mathbf{r}; \mathbf{R}'_{\perp}, 0) = \psi_{0}(\mathbf{R}_{\perp}, \mathbf{r}_{\perp}) \bar{\psi}_{0}(\mathbf{R}'_{\perp}, 0) \frac{i\mu}{k} e^{ik|z|} + \int_{0}^{\infty} dt \, e^{Et} \widetilde{G}_{t}(\mathbf{R}_{\perp}, \mathbf{r}; \mathbf{R}'_{\perp}, 0), \quad (17)$$

where we used Eq. (11) and we explicitly separated the contribution from the open channel. Note that G_t is simply obtained by subtracting from the sum in Eq. (15) the open-channel contributions, i.e., the term with $n_1 = n_2 = 0$ in our case. In the limit $\mathbf{r} \to 0$, we can once again impose the boundary conditions in Eq. (8) and obtain the following integral equation for $f(\mathbf{R}_{\perp})$:

$$-\frac{f(\mathbf{R}_{\perp})}{4\pi a} = \int_{\mathbb{R}^2} d\mathbf{R}_{\perp}' \, \widetilde{\zeta}_E(\mathbf{R}_{\perp}, \mathbf{R}_{\perp}') f(\mathbf{R}_{\perp}') + \psi_0(\mathbf{R}_{\perp}, 0)$$
$$+ \frac{i\psi_0(\mathbf{R}_{\perp}, 0)}{2k} \int_{\mathbb{R}^2} d\mathbf{R}_{\perp}' \, \bar{\psi}_0(\mathbf{R}_{\perp}', 0) f(\mathbf{R}_{\perp}'), \quad (18)$$

where we defined the integral kernel

$$\widetilde{\zeta}_{E}(\mathbf{R}_{\perp}, \mathbf{R}'_{\perp}) = \lim_{r \to 0} \frac{1}{2\mu} \left[\widetilde{G}_{E}(\mathbf{R}_{\perp}, \mathbf{r}; \mathbf{R}'_{\perp}, 0) - \delta(\mathbf{R}_{\perp} - \mathbf{R}'_{\perp}) \frac{\mu}{2\pi r} \right], (19)$$

with \widetilde{G}_E being the closed-channel contribution to the Green's function, i.e., the second line of Eq. (17). Note that we can absorb the term proportional to the Dirac delta in the definition of $\widetilde{\zeta}_E$ inside the time integral. We do that by writing

$$\frac{\mu}{2\pi r} = \int_0^\infty dt \left(\frac{\mu}{2\pi t}\right)^{3/2} e^{-r^2\mu/(2t)},\tag{20}$$

which gives

$$\widetilde{\zeta}_{E}(\mathbf{R}_{\perp}, \mathbf{R}'_{\perp}) = \int_{0}^{\infty} \frac{dt}{2\mu} \left[e^{Et} \widetilde{G}_{t}(\mathbf{R}_{\perp}, 0; \mathbf{R}'_{\perp}, 0) - \left(\frac{\mu}{2\pi t} \right)^{3/2} \delta(\mathbf{R}_{\perp} - \mathbf{R}'_{\perp}) \right]. \tag{21}$$

We refer to Sec. III B for the explicit derivation of \widetilde{G}_t in the case of harmonic confinement and to the Appendix for the computation of the matrix elements of $\widetilde{\zeta}_E$.

In order to understand how $\widetilde{\zeta}_E$ is related to the scattering properties, we now expand Eq. (18) in the basis $|j\rangle$ defined by

$$|f\rangle = \sum_{j} f_{j}|j\rangle, \quad f_{j} = \int_{\mathbb{R}^{2}} d\mathbf{R}_{\perp} \langle j|\mathbf{R}_{\perp} \rangle f(\mathbf{R}_{\perp}), \quad (22)$$

with the ground state defined by $\langle \mathbf{R}_{\perp}|0\rangle = c \,\psi_0(\mathbf{R}_{\perp},0)$, where c is a normalization constant. We can then write Eq. (18) in a compact form:

$$-\frac{|f\rangle}{4\pi a} = \frac{|0\rangle}{c} + \frac{i}{2k} \frac{|0\rangle}{c^2} \langle 0|f\rangle + \widetilde{\zeta}_E |f\rangle, \tag{23}$$

whose formal solution is given by

$$|f\rangle = \frac{-1/c}{1 - i/(ka_{1D})} \left(\widetilde{\zeta}_E + \frac{1}{4\pi a} \right)^{-1} |0\rangle, \tag{24}$$

with

$$a_{\rm 1D} = -\frac{2c^2}{\langle 0|[\widetilde{\zeta}_E + 1/(4\pi a)]^{-1}|0\rangle}.$$
 (25)

To check that this can, indeed, be identified with the 1D scattering length, we consider the solution for a large separation in the longitudinal direction z. In this limit, the contribution from the open channel dominates in Eq. (17), and Eq. (9) gives the scattering solution

$$\Psi(\mathbf{R}_{\perp}, \mathbf{r}) = \psi_0(\mathbf{R}_{\perp}, \mathbf{r}_{\perp}) [e^{ikz} + f_e(k)e^{ik|z|}], \qquad (26)$$

with the even scattering amplitude

$$f_e(k) = \frac{i}{2k} \int_{\mathbb{R}^2} d\mathbf{R}'_{\perp} \bar{\psi}_0(\mathbf{R}'_{\perp}, 0) f(\mathbf{R}'_{\perp}). \tag{27}$$

Using Eq. (24) and the definition of the basis in Eq. (22), we get $f_e(k) = -1/(1 + ika_{1D})$, showing that the term a_{1D} assumes the role of the 1D scattering length. We can therefore describe the effective atom-atom interaction with a 1D potential

$$V_{1D} = g_{1D}\delta(z - z'), \tag{28}$$

with interaction strength $g_{1D} = -1/(\mu a_{1D})$. Indicating by λ_n the eigenvalues of ζ_E and by $|e_n\rangle$ its eigenvectors, we can write

$$g_{1D} = \frac{1}{2\mu c^2} \sum_{n} \frac{|\langle 0|e_n \rangle|^2}{\lambda_n + 1/(4\pi a)}.$$
 (29)

$$\langle \mathbf{x}_{\perp,i}|e^{-H_{\perp}^{(i)}t}|\mathbf{x}_{\perp,i}'\rangle = \frac{m_i\omega_{\perp,i}}{\pi} \frac{e^{-\omega_{\perp,i}t}}{1 - e^{-2\omega_{\perp,i}t}} \exp\left[2m_i\omega_{\perp,i} \frac{e^{-\omega_{\perp,i}t}}{1 - e^{-2\omega_{\perp,i}t}} \mathbf{x}_{\perp,i} \cdot \mathbf{x}_{\perp,i}' - m_i\omega_{\perp,i} \left(\frac{1}{2} + \frac{e^{-2\omega_{\perp,i}t}}{1 - e^{-2\omega_{\perp,i}t}}\right) \left(\mathbf{x}_{\perp,i}^2 + \mathbf{x}_{\perp,i}'^2\right)\right].$$

Now, the transverse propagator for the two particles is obtained as the product of the two single-particle propagators. This can be written in a convenient form when $z \to 0$. In this limit, the two particles are on top of each other, and $\mathbf{x}_{\perp,i}$ \mathbf{R}_{\perp} , where \mathbf{R}_{\perp} is the transverse center-of-mass coordinate. Using the definitions $\ell_{\perp,i} = 1/\sqrt{m_i \omega_{\perp,i}}$,

$$\ell_{M} = \frac{1}{\sqrt{m_{1}\omega_{\perp,1} + m_{2}\omega_{\perp,2}}}, \quad \beta = \frac{\ell_{M}^{2}}{\ell_{\perp,1}^{2}},$$

$$f(t) = \beta \coth(\omega_{\perp,1}t) + (1 - \beta)\coth(\omega_{\perp,2}t),$$

$$g(t) = \beta \frac{1}{\sinh(\omega_{\perp,1}t)} + (1 - \beta) \frac{1}{\sinh(\omega_{\perp,2}t)}, \quad (33)$$

the propagator in the transversal direction can be written in the following compact form:

$$\begin{split} &\prod_{i=1,2} \langle \mathbf{x}_{\perp,i} | e^{-H_{\perp}^{(i)}t} | \mathbf{x}_{\perp,i}' \rangle \\ &= \frac{e^{-\omega_{\perp,1}t}}{1 - e^{-2\omega_{\perp,1}t}} \frac{e^{-\omega_{\perp,2}t}}{1 - e^{-2\omega_{\perp,2}t}} \\ &\times \frac{\beta(1-\beta)}{\pi^2 \ell_M^4} \exp\biggl[-f(t) \frac{\mathbf{R}_{\perp}^2 + \mathbf{R}_{\perp}'^2}{2\ell_M^2} + g(t) \frac{\mathbf{R}_{\perp} \cdot \mathbf{R}_{\perp}'}{\ell_M^2} \biggr]. \end{split} \tag{34}$$

From this definition, we observe that one resonance appears for each eigenvalue λ_n , provided that the overlap between the corresponding eigenvector and the ground state of the basis does not vanish.

B. Harmonic confinement

Let us consider the case of harmonic confinement. We indicate with $\omega_{\perp,i}$ the transverse frequency corresponding to particle i, and we consider the general case where $\omega_{\perp,1} \neq$ $\omega_{\perp,2}$. The single-particle transverse propagator in Eq. (14) can be written as the product of two sums along x_i and y_i , with wave functions $\psi_{n_i}^{(i)}$ and energies E_{n_i} given by the eigenstates and eigenenergies of the 1D harmonic oscillator in the corresponding direction. Dropping all the indices for brevity, we have $E_n = \omega_{\perp}(n+1/2)$ and

$$\psi_n(x) = \frac{1}{\sqrt{2^n n!}} \left(\frac{m\omega_\perp}{\pi}\right)^{\frac{1}{4}} e^{-\frac{m\omega_\perp}{2}x^2} H_n[\sqrt{m\omega_\perp} x], \quad (30)$$

where H_n are Hermite polynomials. The contribution from each direction is computed by using the following identity [28]:

$$\sum_{n=0}^{\infty} \frac{1}{2^n n!} H_n(x) H_n(x') \xi^n$$

$$= \frac{1}{\sqrt{1 - \xi^2}} \exp\left[\frac{2x x' \xi - (x^2 + x'^2) \xi^2}{1 - \xi^2}\right], \quad (31)$$

where $\xi = \exp(-\omega_{\perp}t)$ in our case. The product of the two directions gives

$$\frac{1}{t}\mathbf{x}_{\perp,i}\cdot\mathbf{x}'_{\perp,i} - m_i\omega_{\perp,i}\left(\frac{1}{2} + \frac{e^{-2\omega_{\perp,i}t}}{1 - e^{-2\omega_{\perp,i}t}}\right)\left(\mathbf{x}_{\perp,i}^2 + \mathbf{x}'_{\perp,i}^2\right)\right]. \tag{32}$$

As we mentioned in Sec. III A, when the lowest channel is open, we need to separate its contribution from Eq. (34). This is done by subtracting the term corresponding to $n_x = n_y =$ 0 for the two particles. Combining the previous results and considering the longitudinal propagator in Eq. (13) in the limit $z, z' \rightarrow 0$, we obtain the imaginary-time propagator projected onto the Hilbert space of closed channels:

$$\widetilde{G}_{t}(\mathbf{R}_{\perp}, 0; \mathbf{R}'_{\perp}, 0)
= \sqrt{\frac{\mu}{2\pi t}} \frac{\beta(1-\beta)}{\pi^{2} \ell_{M}^{4}} \left\{ \frac{\exp\left[-f(t) \frac{\mathbf{R}_{\perp}^{2} + \mathbf{R}'_{\perp}^{2}}{2\ell_{M}^{2}} + g(t) \frac{\mathbf{R}_{\perp} \cdot \mathbf{R}'_{\perp}}{\ell_{M}^{2}}\right]}{(1 - e^{-2\omega_{\perp,1}t})(1 - e^{-2\omega_{\perp,2}t})}
- \exp\left[-\frac{\mathbf{R}_{\perp}^{2} + \mathbf{R}'_{\perp}^{2}}{2\ell_{M}^{2}}\right] \right\} e^{-(\omega_{\perp,1} + \omega_{\perp,2})t}.$$
(35)

The previous equation is used in Eq. (21) to obtain ζ_E . The latter is then diagonalized to obtain the 1D interaction strength g_{1D} , as discussed in the previous section, with the normalization constant given by $c = \sqrt{\pi} \ell_1 \ell_2 / \ell_M$ in the case of harmonic confinement. The calculation of the matrix elements of ζ_E is detailed in the Appendix.

IV. SPECTRUM IN THE 1D LIMIT

Here, we consider the system described in Sec. II in the limit where the transversal trapping is infinitely tight and the particles are forced to move in the longitudinal direction. The longitudinal confinement of the two species, which was previously neglected, is now taken into account and is represented by a harmonic potential with frequencies ω_1 and ω_2 . In this scenario, the atom-atom interaction is modeled by a one-dimensional contact potential.

The energy spectrum as a function of the 1D scattering length can be computed similarly to that in Ref. [29]. The 1D Hamiltonian is written in terms of the center-of-mass (Z, P_z) and relative coordinates (z, p_z) as

$$H_{1D} = H_{\text{com}} + H_{\text{rel}} + \kappa zZ. \tag{36}$$

The first and second terms on the right-hand side correspond to the Hamiltonian of the center-of-mass and relative harmonic oscillator:

$$H_{\text{com}} = \frac{P_z^2}{2M} + \frac{M\Omega^2}{2} Z^2,$$

$$H_{\text{rel}} = \frac{p_z^2}{2\mu} + \frac{\mu\omega^2}{2} z^2 + V_{\text{1D}}(z),$$
(37)

where $V_{\rm 1D}(z)$ is defined in Eq. (28). The frequencies are given by

$$\Omega = \omega_1 \sqrt{\frac{1+\lambda}{1+\sigma}}, \quad \omega = \omega_1 \sqrt{\frac{\sigma^2 + \lambda}{\sigma(1+\sigma)}},$$
 (38)

with $\sigma = m_2/m_1$ and $\lambda = m_2\omega_2^2/(m_1\omega_1^2)$. The last term in Eq. (36) is the coupling between the center of mass and relative motion with the coupling coefficient

$$\kappa = m_1 \omega_1^2 \frac{\sigma - \lambda}{1 + \lambda}.\tag{39}$$

Note that $\omega_1 = \omega_2$ implies $\kappa = 0$, meaning that the center of mass and relative motion separate in that case. It is convenient to write the matrix elements of H_{1D} in the basis given by the product states:

$$\Psi_{Nn}(Z,z) = \Phi_N(Z)\varphi_n(z), \tag{40}$$

with $\Phi_N(Z)$ and $\varphi_n(z)$ being the eigenstates of H_{com} and H_{rel} , respectively. For every N, $\Phi_N(Z)$ is simply given by Eq. (30) with the appropriate frequency and mass. On the other hand, $\varphi_n(z)$ is given by the same expression only when n is odd, in which case it vanishes at z=0 and the contact interaction has no effect. When n is even, the relative wave functions are perturbed by the interaction potential and are given by

$$\varphi_n(x) = A_n e^{-\frac{\mu\omega}{2}z^2} U\left(-\frac{\nu_n}{2}, \frac{1}{2}, \mu\omega z^2\right),$$
 (41)

where A_n is a normalization factor and U(a, b, z) is the Tricomi confluent hypergeometric function. The corresponding eigenvalue is given by $\varepsilon_n = \omega(\nu_n + 1/2)$ (see Fig. 2), where ν_n is the noninteger solution to the equation [30]

$$\frac{\Gamma(-\varepsilon_n/2 + 1/4)}{2\Gamma(-\varepsilon_n/2 + 3/4)} = a_{1D},\tag{42}$$

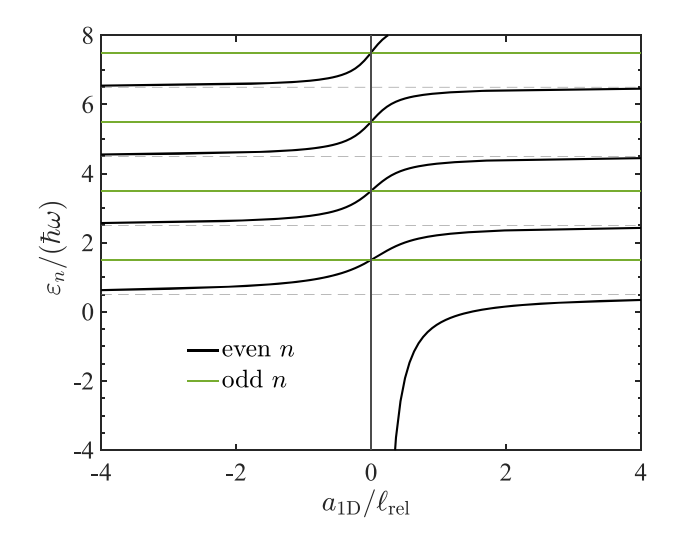


FIG. 2. Energy spectrum of $H_{\rm rel}$ as a function of the 1D scattering length. Thick black lines: energies for even n approaching the non-interacting values (gray dashed lines) at large negative or positive values of $a_{\rm 1D}$. Thin green lines: energies for odd n. Units are rescaled with respect to the energy $\hbar\omega$ and length $\ell_{\rm rel}=\sqrt{\hbar/(\mu\omega)}$ of the relative harmonic oscillator.

with $\Gamma(z)$ being Euler's gamma function and $a_{\rm 1D}$ being the 1D scattering length. Note that the definition of ν_n can be extended by establishing that $\nu_n = n$ when n is odd. In doing that, the definition in Eq. (41) can be used as a general definition for the relative wavefunction since it retrieves the wave function of the unperturbed harmonic oscillator when ν_n is a positive integer [31]. The matrix elements of $H_{\rm 1D}$ are therefore given by

$$[H_{1D}]_{i,j} = \Omega \left(N_i + \frac{1}{2} \right) \delta_{i,j} + \omega \left(\nu_{n_i} + \frac{1}{2} \right) \delta_{i,j}$$
$$+ \kappa \left\langle \varphi_{n_i}(z) | z | \varphi_{n_j}(z) \right\rangle \left\langle \Phi_{N_i}(Z) | Z | \Phi_{N_j}(Z) \right\rangle, \quad (43)$$

and the energy spectrum is obtained via numerical diagonalization.

V. NUMERICAL ANALYSIS

The following numerical analysis is devoted to the case of harmonic confinement. Moreover, we focus on the ultracold regime where $E \to E_0$ and only the ground state is energetically open. Results are therefore based on the derivations in Secs. III B and IV.

Without loss of generality, we always consider the masses of the two species to be those of ⁸⁷Rb and ⁸⁷Sr, where $m_{\rm Rb} \simeq 86.9092m_u$ and $m_{\rm Sr} \simeq 86.9089m_u$ ($m_u \simeq 1.6605 \times 10^{-27}$ kg). Note that, from this point forward, we will use a subscript 1 to denote quantities related to the strontium atom and a subscript 2 for those related to the rubidium atom.

A. Resonance position

Let us start by studying the position of confinement-induced resonances for different values of the ratio $\omega_{\perp,2}/\omega_{\perp,1}$ in the quasi-1D regime. We recall that in this regime the confinement is purely transversal. In Fig. 3(a), the interaction

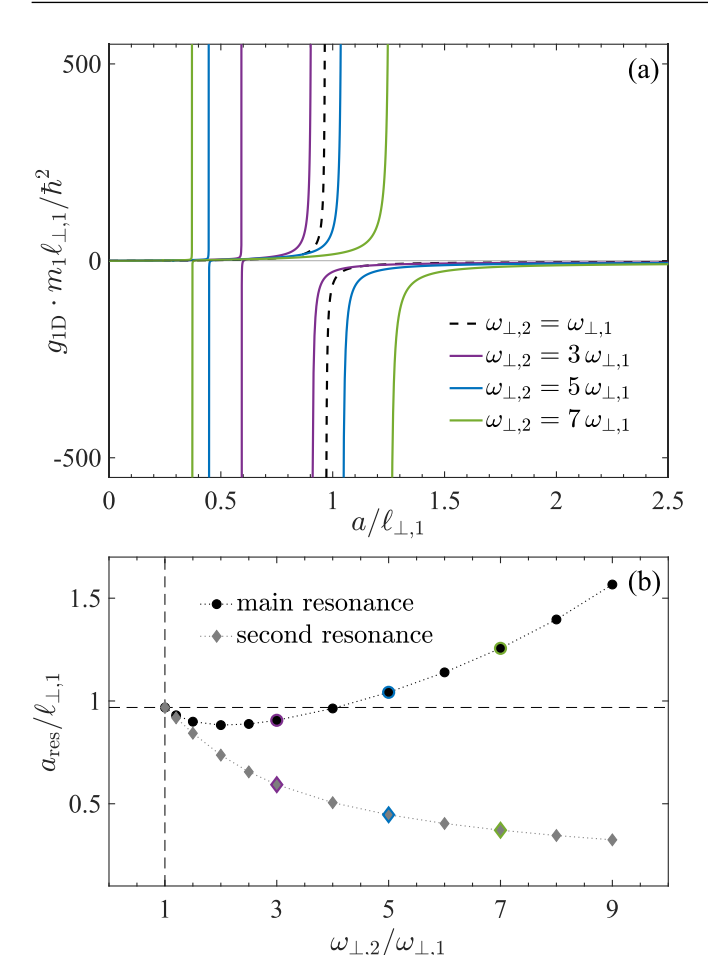


FIG. 3. Confinement-induced resonances for different frequency ratios. (a) Interaction strength g_{1D} as a function of scattering length. (b) Values a_{res} of scattering length a for which the main (black circles) and second resonance (gray diamonds) appear. Dashed lines indicate the analytical value obtained for $\omega_{\perp,2} = \omega_{\perp,1}$. The positions of the resonances shown in (a) are highlighted with the corresponding color. Dotted lines are only a guide to the eye.

strength g_{1D} as defined in Eq. (29) is plotted as a function of the 3D scattering length a for different values of the trap frequency ratio $\omega_{\perp,2}/\omega_{\perp,1}$. We observe that in the case where $\omega_{\perp,2}=\omega_{\perp,1}$ (black dashed line), only one resonance appears. This can be interpreted as a zero-energy Feshbach resonance due to the binding energy of the first excited relative-motion state matching the continuum threshold of the open channel [16,17]. The position of this resonance is computed analytically in Ref. [15].

As the frequency ratio deviates from unity, an additional narrow resonance appears for lower values of a. Figure 3(b) shows the values $a_{\rm res}$ of a at which the main and second resonances in $g_{\rm 1D}$ are located for different ratios. We observe that the position of the second resonance (gray diamonds) decreases as $\omega_{\perp,2}/\omega_{\perp,1}$ increases. Like in the case with equal traps, this resonance has a Feshbach-like interpretation. In this case, however, it is related to the first excited center-of-mass bound state. Note that, in principle, a distinct resonance is associated with each of the higher excited center-of-mass states. However, their width is vanishing in the range of values

that we consider for the trap ratio. The position of the main resonance (black circles), on the other hand, presents a minimum around $\omega_{\perp,2}=2\,\omega_{\perp_1}$ and does not have a similar interpretation. We can therefore speculate that the state responsible for its presence is a nontrivial combination of center-of-mass and relative bound states.

B. Spectrum of the ⁸⁷Rb - ⁸⁷Sr mixture

We now consider the specific case where 87 Rb and 87 Sr are confined by the same optical dipole potential. Due to their different polarizabilities, the two species experience distinct trapping frequencies. Specifically, at the commonly used optical trap wavelength of 1064 nm, the resulting trap frequency ratio is $\omega_{(\perp),2} \simeq 1.82\omega_{(\perp),1}$ for both the transverse and longitudinal directions. Combining the results derived in Secs. III and IV, we compute the 1D spectrum as a function of the 3D scattering length a. This is done by mapping a to a_{1D} using Eq. (29) and diagonalizing the Hamiltonian in Eq. (43).

In Figs. 4(a) and 4(b), we present the spectrum and the corresponding values of the 1D scattering length, respectively. They are plotted as a function of the ratio between a and the oscillator length associated with the perpendicular confinement of strontium atoms $\ell_{\perp,1}$, as shown in the lower axis of Fig. 4(b). The upper axis of Fig. 4(a) indicates the corresponding dependence on the frequency $\omega_{\perp,1}$, which is accessible experimentally and is computed from the ratio $a/\ell_{\perp,1}$ by considering the scattering length $a_{Rb-Sr} = 1420a_0$ between 87 Rb and 87 Sr in units of the Bohr radius a_0 . We observe that the avoided crossings between trapped states and excited bound states are found in a narrow range of values around $\omega_{\perp,1} = 12.418 \,\mathrm{kHz}$ (dotted vertical line), where a_{1D} has a pole and the spectrum crosses the asymptotic noninteracting states (dashed horizontal lines). To better understand these features, we recall that the scattering length in the 1D limit is inversely proportional to the interaction strength. Hence, large variations of a_{1D} are obtained with small variations of g_{1D} around zero. From Figs. 4(c) and 4(d), it is evident that this can be achieved only in the region between the two poles in g_{1D} , where the latter crosses the horizontal axes and a_{1D} presents a narrow resonance. Figure 2 shows that for large positive values of a_{1D} , the relative Hamiltonian supports a shallow molecular bound state. We propose that such a bound state may be populated by adiabatically ramping the system toward smaller values of $\omega_{\perp,1}$, thus transferring atoms into the molecular bound state. A possible pathway is indicated by the red arrow in Fig. 4(a). The transfer efficiency is expected to be high when the ramping timescales are long compared to $1/\omega_1$, such that the system is allowed to adiabatically follow the ground state in Fig. 4(a). It is worth noting that additional crossings between bound states and trapped states occur in the range where $a/\ell_{\perp,1} \lesssim 5$, i.e., $\omega_{\perp,1} \lesssim 700 \, \text{kHz}$, which is much more challenging to access in current experiments. Furthermore, it is important to recognize that the reported resonance position is found by assuming $a_{Rb-Sr} = 1420 a_0$. Experimental realizations should account for the uncertainty in a_{Rb-Sr} and its impact on this estimate.

We finally remark that these results are relevant for ongoing experiments involving the creation of weakly bound

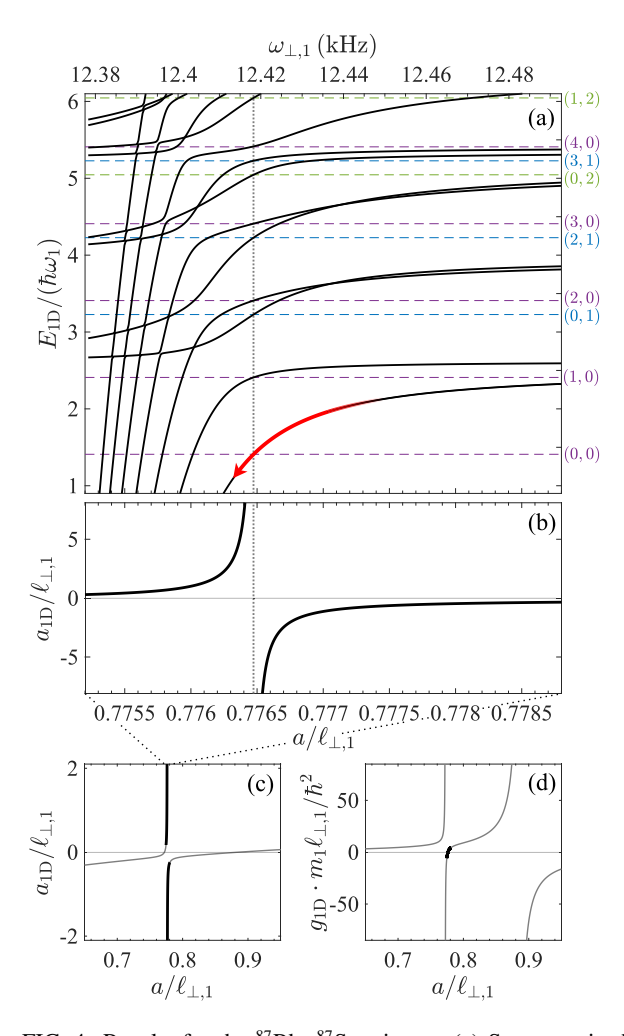


FIG. 4. Results for the ⁸⁷Rb - ⁸⁷Sr mixture. (a) Spectrum in the 1D limit. The upper axis indicates the transverse strontium frequency $\omega_{\perp,1}$ considering the fixed interspecies scattering length $a_{\rm Sr-Rb} =$ $1420a_0$ (a_0 is the Bohr radius). Horizontal dashed lines correspond to the asymptotic noninteracting states for different values of (n_1, n_2) , as indicated on the right side of the plot, with n_1 and n_2 being the principal quantum numbers of the longitudinal harmonic oscillators of strontium and rubidium, respectively. Purple lines are for $n_2 = 0$, blue lines are for $n_2 = 1$, and green lines are for $n_2 = 2$. The vertical dotted line indicates the position of the resonance of a_{1D} appearing at $\omega_{\perp,1}=12.418\,\mathrm{kHz}$ or $a=0.77647\ell_{\perp,1}$ ($\ell_{\perp,1}$ is the length associated with $\omega_{\perp,1}$). The red arrow indicates a possible pathway for dimer formation: The system is prepared on the right side of the resonance and adiabatically ramped across it to populate a bound state. (b) 1D scattering length $a_{1D} = -1/(\mu g_{1D})$ in units of $\ell_{\perp,1}$. The bottom axis indicates the 3D scattering length in units of $\ell_{\perp,1}$. (c) 1D scattering length on a broader range. (d) 1D interaction strength g_{1D} . The values used in previous plots are highlighted in black.

⁸⁷Rb - ⁸⁷Sr dimers. In particular, the spectrum in Fig. 4(a) reveals the coupling between excited bound states and lowerlying trapped states. CIRs can therefore be exploited to adiabatically ramp the system from a regime where the two species are in their corresponding unbound trapped state to the one where bound states are occupied. We refer to the next section for a comment on this matter.

VI. RELATION TO EXPERIMENTS

In this section, we examine the experimental conditions necessary for observing confinement-induced resonances in ⁸⁷Rb - ⁸⁷Sr mixtures and explore their potential as a pathway for the formation of weakly bound dimers.

First, we remark that the observation of CIRs requires a near-threshold molecular bound state with a binding energy comparable to the harmonic trapping frequency. The selection of the ⁸⁷Rb-⁸⁷Sr isotopologue is motivated by the existence of such a bound state, with a binding energy of approximately 20 kHz, well matched to typical trap frequencies achievable in state-of-the-art optical dipole traps and optical lattices [32]. Tuning the harmonic trapping frequency across a CIR is particularly important in ultracold mixtures with narrow Feshbach resonances, as it enables controlled coupling between the near-threshold bound state and the trapped atomic states.

This requirement narrows the range of suitable experimental platforms for studying CIRs in quasi-one-dimensional regimes. Two main approaches are particularly relevant: The first employs a two-dimensional optical lattice to create tightly confining, tubelike dipole potentials, effectively restricting motion to one dimension. The second consists of using optical tweezers for precise control of individual atoms or small ensembles in highly anisotropic traps. Both methods offer excellent tunability of dimensionality and interaction parameters, providing ideal conditions for observing CIRs.

However, in the ⁸⁷Rb - ⁸⁷Sr system, the near-threshold bound state results in a large three-dimensional scattering length of approximately 1420*a*₀, leading to strong interspecies interactions and rapid three-body recombination losses. Sympathetic cooling in overlapping traps is therefore inefficient. To address this limitation, the atomic species undergo independent evaporative cooling in spatially separated optical dipole traps before being adiabatically merged into a common quasi-one-dimensional confinement potential. This sequential cooling strategy minimizes interspecies collisions during critical evaporative stages while preserving phase-space density.

The detection of CIRs can be achieved by monitoring atomic loss rates due to enhanced three-body recombination near resonance, although this method becomes less sensitive in quasi-1D systems due to the suppression of three-body recombination in one dimension [33]. More precise detection involves measuring interspecies thermalization rates, which increase near a CIR as the effective one-dimensional scattering length diverges [34]. Alternatively, photoassociation spectroscopy can be employed, where resonantly enhanced atom-molecule coupling leads to increased photoassociation rates near resonance.

Based on these considerations, confinement-induced resonances are expected to provide a promising route toward the formation of weakly bound ⁸⁷Rb - ⁸⁷Sr dimers.

VII. CONCLUSIONS

We studied the emergence of confinement-induced resonances in ultracold mixtures of two atomic species trapped by harmonic quasi-1D potentials with mismatched trapping frequencies. We systematically analyzed the behavior of CIRs and their dependence on the ratio between the transverse

trapping frequencies $\omega_{\perp,2}/\omega_{\perp,1}$ of the two species (Fig. 3). In the case of equal frequencies, it is a well-known result (see Ref. [15]) that a single resonance appears. Our results show that an additional narrow resonance attached to the first excited center-of-mass bound state emerges at smaller values of the scattering length when the frequencies are different. Resonances attached to higher center-of-mass excited states are vanishingly narrow for the considered values of the frequency ratio. Furthermore, we focused on the case where ⁸⁷Rb and ⁸⁷Sr are confined in the same trap, resulting in $\omega_{(\perp),2}/\omega_{(\perp),1} \simeq 1.82$ along all directions. The energy spectrum as a function of the transverse frequency of strontium atoms suggests that ⁸⁷Rb - ⁸⁷Sr dimers can be created by properly ramping the system through a resonance that appears in the 1D scattering length at $\omega_{\perp,1} = 12.418 \, \text{kHz}$ (Fig. 4).

This work provides a theoretical framework for the efficient formation of ultracold gases of ⁸⁷Rb-⁸⁷Sr dimers. In doing so, it paves the way for extending the approach to other alkali–alkaline-earth atomic mixtures. Additionally, possible future extensions involve developing an analogous analysis for quasi-two-dimensional geometries.

ACKNOWLEDGMENTS

A.S.-N. was supported by the Dutch Research Council (NWO/OCW) as a part of the Quantum Software Consortium (Project No. 024.003.037), Quantum Delta NL (Project No. NGF.1582.22.030), and an ENW-XL grant (Project No. OCENW.XL21.XL21.122). N.P.M. and S.T.R. acknowledge support from the National Science Foundation through ITAMP and in part through NSF Grant No. 2409110 and from Quantum Delta NL through the University of Amsterdam. P.T. was supported by the Dutch Research Council (NWO) as part of Quantum Simulation 2.0 (Grant No. 680.92.18.05) and by the Novo Nordisk Foundation (Grant No. NNF23OC0086815).

DATA AVAILABILITY

The data that support the findings of this article are not publicly available upon publication because it is not technically feasible and/or the cost of preparing, depositing, and hosting the data would be prohibitive within the terms of this research project. The data are available from the authors upon reasonable request.

APPENDIX: MATRIX ELEMENTS OF $\tilde{\zeta}_E$ FOR HARMONIC CONFINEMENT

Here, we calculate the matrix elements of the operator ζ_E as defined in Eq. (21). To do that, we consider the basis

$$\langle \mathbf{R}_{\perp} | n_x, n_y \rangle = \frac{1}{\ell_M} \psi_{n_x} \left(\frac{R_{\perp}^{(x)}}{\ell_M} \right) \psi_{n_y} \left(\frac{R_{\perp}^{(y)}}{\ell_M} \right), \quad (A1)$$

where ψ_n indicates the 1D harmonic oscillator wave function in Eq. (30), $R_{\perp}^{(x)}$ is the first component of the center-of-mass coordinate, and ℓ_M is defined in Eq. (33).

We start from the matrix elements of \widetilde{G}_t :

$$\begin{split} [\widetilde{G}(t)]_{\mathbf{n},\mathbf{m}} &\equiv \langle n_x, n_y | \widetilde{G}_t(\mathbf{R}_\perp, 0; \mathbf{R}'_\perp, 0) | m_x, m_y \rangle \\ &= \sqrt{\frac{\mu}{2\pi t}} \frac{\beta(1-\beta)}{\pi^2 \ell_M^2} e^{-(\omega_{\perp,1} + \omega_{\perp,2})t} \\ &\times \left\{ \frac{[\widetilde{F}(t)]_{n_x, m_x} [\widetilde{F}(t)]_{n_y, m_y}}{(1 - e^{-2\omega_{\perp,1}t})(1 - e^{-2\omega_{\perp,2}t})} - \pi \, \delta_{\mathbf{n},0} \delta_{\mathbf{m},0} \right\}, \end{split}$$
(A2)

where we defined

$$[\widetilde{F}(t)]_{n,m} = \int_{-\infty}^{\infty} dX \int_{-\infty}^{\infty} dX' \, \bar{\psi}_n(X) \psi_m(X')$$

$$\times \exp\left[-\frac{f(t)}{2} (X^2 + X'^2) + g(t) X X' \right]$$

$$= \int_{-\infty}^{\infty} dX \int_{-\infty}^{\infty} dX' \, \frac{H_n(X) H_m(X')}{\sqrt{\pi 2^{n+m} n! m!}}$$

$$\times \exp\left[-\frac{1 + f(t)}{2} (X^2 + X'^2) + g(t) X X' \right]$$
(A3)

and the rescaled coordinate $X = R_{\perp}^{(x)}/\ell_M$. Definitions along y are analogous. Note that in the second equality, we explicitly used the 1D harmonic oscillator eigenstates. The integral over X is computed by means of the identity [28]

$$\int_{-\infty}^{\infty} dz \, e^{-(z-z')^2} H_n(\alpha z) = \sqrt{\pi} (1 - \alpha^2)^{\frac{n}{2}} H_n \left[\frac{\alpha z'}{\sqrt{1 - \alpha^2}} \right],\tag{A4}$$

with $\alpha(t) = \{2/[1+f(t)]\}^{1/2}$, $z = X/\alpha(t)$, and $z' = g(t)\alpha(t)X'/2$. Completing the square in the exponential in Eq. (A3), we are left with

$$[\widetilde{F}(t)]_{n,m} = \frac{\alpha (1 - \alpha^2)^{\frac{n}{2}}}{\sqrt{2^{n+m} n! m!}} \int_{-\infty}^{\infty} dX' H_m(X')$$

$$\times H_n \left(\frac{g\alpha^2}{2\sqrt{1 - \alpha^2}} X' \right) \exp\left[-X'^2 \left(\frac{1}{\alpha^2} - \frac{g^2 \alpha^2}{4} \right) \right],$$
(A5)

which can be computed using the following identity [35]:

$$\int_{-\infty}^{\infty} dy \, e^{-y^2} H_n(py) H_m(qy) = 2^{2M} \Gamma\left(M + \frac{1}{2}\right) \gamma^n \delta^m$$

$$\times {}_2F_1\left(-n, -m; -M + \frac{1}{2}; \frac{\gamma \delta - pq}{2\gamma \delta}\right), \tag{A6}$$

with 2M = m + n, $\gamma^2 = p^2 - 1$, $\delta^2 = q^2 - 1$, and ${}_2F_1$ being the hypergeometric function. To use this identity in Eq. (A5), we define $y = X'(1/\alpha^2 - g^2\alpha^2/4)^{1/2}$, and we perform the change of variable $X' \to y$. Finally, we can write the expression for the matrix element of $\widetilde{\zeta}_E$:

$$[\widetilde{\zeta}_E]_{\mathbf{n},\mathbf{m}} = \frac{1}{2\mu} \int_0^\infty dt \left\{ e^{Et} [\widetilde{G}_t]_{\mathbf{n},\mathbf{m}} - \left(\frac{\mu}{2\pi t}\right)^{\frac{3}{2}} \delta_{\mathbf{n},\mathbf{m}} \right\}.$$
(A7)

- [1] T. Langen, G. Valtolina, D. Wang, and J. Ye, Quantum state manipulation and cooling of ultracold molecules, Nat. Phys. **20**, 702 (2024).
- [2] A. Micheli, G. K. Brennen, and P. Zoller, A toolbox for lattice-spin models with polar molecules, Nat. Phys. 2, 341 (2006).
- [3] T. S. Roussy, L. Caldwell, T. Wright, W. B. Cairncross, Y. Shagam, K. B. Ng, N. Schlossberger, S. Y. Park, A. Wang, J. Ye, and E. A. Cornell, An improved bound on the electron's electric dipole moment, Science 381, 46 (2023).
- [4] D. DeMille, N. R. Hutzler, A. M. Rey, and T. Zelevinsky, Quantum sensing and metrology for fundamental physics with molecules, Nat. Phys. **20**, 741 (2024).
- [5] J. L. Bohn, A. M. Rey, and J. Ye, Cold molecules: Progress in quantum engineering of chemistry and quantum matter, Science 357, 1002 (2017).
- [6] B. K. Stuhl, B. C. Sawyer, D. Wang, and J. Ye, Magneto-optical trap for polar molecules, Phys. Rev. Lett. **101**, 243002 (2008).
- [7] E. S. Shuman, J. F. Barry, and D. DeMille, Laser cooling of a diatomic molecule, Nature (London) 467, 820 (2010).
- [8] D. Mitra, N. B. Vilas, C. Hallas, L. Anderegg, B. L. Augenbraun, L. Baum, C. Miller, S. Raval, and J. M. Doyle, Direct laser cooling of a symmetric top molecule, Science 369, 1366 (2020).
- [9] V. Jorapur, T. K. Langin, Q. Wang, G. Zheng, and D. DeMille, High density loading and collisional loss of laser-cooled molecules in an optical trap, Phys. Rev. Lett. 132, 163403 (2024).
- [10] K.-K. Ni, S. Ospelkaus, M. H. G. de Miranda, A. Pe'er, B. Neyenhuis, J. J. Zirbel, S. Kotochigova, P. S. Julienne, D. S. Jin, and J. Ye, A high phase-space-density gas of polar molecules, Science 322, 231 (2008).
- [11] J. G. Danzl, E. Haller, M. Gustavsson, M. J. Mark, R. Hart, N. Bouloufa, O. Dulieu, H. Ritsch, and H.-C. Nägerl, Quantum gas of deeply bound ground state molecules, Science 321, 1062 (2008).
- [12] T. Takekoshi, L. Reichsöllner, A. Schindewolf, J. M. Hutson, C. R. Le Sueur, O. Dulieu, F. Ferlaino, R. Grimm, and H.-C. Nägerl, Ultracold dense samples of dipolar RbCs molecules in the rovibrational and hyperfine ground state, Phys. Rev. Lett. 113, 205301 (2014).
- [13] C. Chin, R. Grimm, P. Julienne, and E. Tiesinga, Feshbach resonances in ultracold gases, Rev. Mod. Phys. 82, 1225 (2010).
- [14] A. Ciamei, S. Finelli, A. Trenkwalder, M. Inguscio, A. Simoni, and M. Zaccanti, Exploring ultracold collisions in ⁶Li-⁵³Cr Fermi mixtures: Feshbach resonances and scattering properties of a novel alkali-transition metal system, Phys. Rev. Lett. 129, 093402 (2022).
- [15] M. Olshanii, Atomic scattering in the presence of an external confinement and a gas of impenetrable bosons, Phys. Rev. Lett. 81, 938 (1998).
- [16] T. Bergeman, M. G. Moore, and M. Olshanii, Atom-atom scattering under cylindrical harmonic confinement: Numerical and analytic studies of the confinement induced resonance, Phys. Rev. Lett. 91, 163201 (2003).
- [17] V. Peano, M. Thorwart, C. Mora, and R. Egger, Confinement-induced resonances for a two-component ultracold atom gas in arbitrary quasi-one-dimensional traps, New J. Phys. 7, 192 (2005).

- [18] E. Haller, M. J. Mark, R. Hart, J. G. Danzl, L. Reichsöllner, V. Melezhik, P. Schmelcher, and H.-C. Nägerl, Confinementinduced resonances in low-dimensional quantum systems, Phys. Rev. Lett. 104, 153203 (2010).
- [19] S. Sala, G. Zürn, T. Lompe, A. N. Wenz, S. Murmann, F. Serwane, S. Jochim, and A. Saenz, Coherent molecule formation in anharmonic potentials near confinement-induced resonances, Phys. Rev. Lett. 110, 203202 (2013).
- [20] S. Sala and A. Saenz, Theory of inelastic confinement-induced resonances due to the coupling of center-of-mass and relative motion, Phys. Rev. A 94, 022713 (2016).
- [21] D. Capecchi, C. Cantillano, M. J. Mark, F. Meinert, A. Schindewolf, M. Landini, A. Saenz, F. Revuelta, and H.-C. Nägerl, Observation of confinement-induced resonances in a 3D lattice, Phys. Rev. Lett. 131, 213002 (2023).
- [22] P. S. Žuchowski, R. Guérout, and O. Dulieu, Ground- and excited-state properties of the polar and paramagnetic RbSr molecule: A comparative study, Phys. Rev. A 90, 012507 (2014).
- [23] P. S. Żuchowski, J. Aldegunde, and J. M. Hutson, Ultracold RbSr molecules can be formed by magnetoassociation, Phys. Rev. Lett. **105**, 153201 (2010).
- [24] D. A. Brue and J. M. Hutson, Prospects of forming ultracold molecules in $^2\Sigma$ states by magnetoassociation of alkali-metal atoms with Yb, Phys. Rev. A **87**, 052709 (2013).
- [25] V. Barbé, A. Ciamei, B. Pasquiou, L. Reichsöllner, F. Schreck, P. S. Żuchowski, and J. M. Hutson, Observation of Feshbach resonances between alkali and closed-shell atoms, Nat. Phys. 14, 881 (2018).
- [26] R. P. Feynman, A. R. Hibbs, and D. F. Styer, *Quantum Mechanics and Path Integrals* (Dover, Mineola, NY, 2010).
- [27] This can be verified by simply integrating $n_1 = n_2 = 0$ in Eq. (15) according to Eq. (11) and by applying the definition of ζ_E in Eq. (19).
- [28] I. Gradshteyn and I. Ryzhik, *Table of Integrals, Series, and Products* (Elsevier, San Diego, CA, 2007).
- [29] J. F. Bertelsen and K. Mølmer, Association of heteronuclear molecules in a harmonic oscillator well, Phys. Rev. A **76**, 043615 (2007).
- [30] T. Busch, B.-G. Englert, K. Rzażewski, and M. Wilkens, Two cold atoms in a harmonic trap, Found. Phys. 28, 549 (1998).
- [31] K. Oldham, J. Myland, and J. Spanier, *An Atlas of Functions* (Springer, New York, NY, 2009).
- [32] A. Ciamei, J. Szczepkowski, A. Bayerle, V. Barbé, L. Reichsöllner, S. M. Tzanova, C.-C. Chen, B. Pasquiou, A. Grochola, P. Kowalczyk, W. Jastrzebski, and F. Schreck, The RbSr ²Σ ground state investigated via spectroscopy of hot and ultracold molecules, Phys. Chem. Chem. Phys. 20, 26221 (2018).
- [33] N. P. Mehta, B. D. Esry, and C. H. Greene, Three-body recombination in one dimension, Phys. Rev. A **76**, 022711 (2007).
- [34] H.-W. Cho, D. J. McCarron, M. P. Köppinger, D. L. Jenkin, K. L. Butler, P. S. Julienne, C. L. Blackley, C. R. Le Sueur, J. M. Hutson, and S. L. Cornish, Feshbach spectroscopy of an ultracold mixture of ⁸⁵Rb and ¹³³Cs, Phys. Rev. A 87, 010703(R) (2013).
- [35] R. D. Lord, Some integrals involving hermite polynomials, J. London Math. Soc. s1-24, 101 (1949).